Analytical Methods

Accepted Manuscript

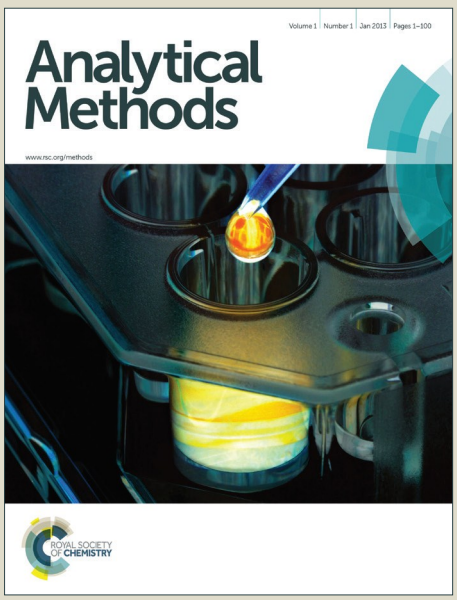

This is an *Accepted Manuscript*, which has been through the Royal Society of Chemistry peer review process and has been accepted for publication.

Accepted Manuscripts are published online shortly after acceptance, before technical editing, formatting and proof reading. Using this free service, authors can make their results available to the community, in citable form, before we publish the edited article. We will replace this *Accepted Manuscript* with the edited and formatted *Advance Article* as soon as it is available.

You can find more information about *Accepted Manuscripts* in the Information for Authors.

Please note that technical editing may introduce minor changes to the text and/or graphics, which may alter content. The journal's standard Terms & Conditions and the Ethical guidelines still apply. In no event shall the Royal Society of Chemistry be held responsible for any errors or omissions in this *Accepted Manuscript* or any consequences arising from the use of any information it contains.

ROYAL SOCIETY OF CHEMISTRY

www.rsc.org/methods

Electrocatalytic oxidation of N–acetyl–L–cysteine at quercetin multiwall carbon nanotubes modified GCE: Application for simultaneous determination of ascorbic acid, L–DOPA, N–acetyl–L–cysteine, acetaminophen and tryptophan

Hamid R. Zare,* Marjan Haji-Dehabadi, Zahra Shekari

Department of Chemistry, Yazd University, Yazd, 89195-741, Iran

Fax number: +98 353 8210991 Telephon number: +98 353 1232669

E-mail address: hrzare@yazd.ac.ir

Abstract

In the present study, a modified electrode has been constructed by immobilizing of quercetin at the surface of a glassy carbon electrode modified with multi–wall carbon nanotubes (Q–MWCNT–GCE), and its electrochemical characteristics were studied by cyclic voltammetry. Q–MWCNT–GCE was successfully used for N–acetyl–L–cysteine (NAC) electrocatalytic oxidation and simultaneous determination of ascorbic acid (AA), L–DOPA (LD), NAC, acetaminophen (AC) and tryptophan (Trp). The obtained results indicate that the peak potential of NAC oxidation at the Q–MWCNT–GCE surface appears at the less positive potential compared with that at the MWCNT–GCE or Q–GCE surface. The electron transfer coefficient, α, and the heterogeneous electron transfer rate constant, k', for the oxidation of NAC at the Q–MWCNT–GCE surface were calculated 0.30 and 6.5×10^{-4} cm s^{-1}, respectively. Furthermore, differential pulse voltammetry (DPV) exhibits two linear dynamic ranges of 1.1–50.0 and 50.0–1000.0 μM and a detection limit of 0.44 μM for NAC determination. Also, Q–MWCNT–GCE was used to simultaneous determination of AA, LD, NAC, AC and Trp with DPV. Finally, the activity of the modified electrode was also investigated for determination of AA, LD, NAC and AC in real samples and satisfactory results were obtained.

1. Introduction

Ascorbic acid (AA) also known as vitamin C, exists in biological systems as blood and urine.[1,2] It acts as an antioxidant on a large scale in foods,animal feed, biological fluids and pharmaceutical formulations.[3,4] Due to the concentration of AA being on a millimolar level in the central nervous system, it has important regulatory effects on neurotransmitters, enzymes and neuropeptides.[5] In addition, vitamin C aiding antioxidant properties also converts glutathione produced from cysteine to its reduced form and because it inhibits oxidation of NAC. Vitamin C supplements are also recommended when taking NAC. So, it is very important to measure the concentration of NAC in the presence of AA.[1] L–DOPA is a naturally occurring dietary supplement and psychoactive drug found in certain kinds of herbs and foods.[6] It precedes the formation (or is a precursor) of three neurotransmitters: dopamine, norepinephrine, and epinephrine and it has been widely used as drug in the medication of neural disorders such as Parkinson's disease, which is caused by a depletion of dopamine in the brain, and dopamine–responsive dystonia.[7,8] Because L–DOPA is a precursor of dopamine, it works by increasing dopamine concentration in the brain since it can cross the blood–brain barrier, and dopamine itself cannot.[9] The previous studies show that the addition of AA effectively reduces Parkinson's disease progression.[10-14]

N–Acetyl–L–cysteine (NAC), precursor of reduced GSH and also one of the homologs of L–cysteine acts as a dietary supplement commonly claiming antioxidant, prospective radiation protector, antitoxin and free radical scavenger and it also has liver protecting effects. It is used to counteract acetaminophen and carbon monoxide poisoning. NAC treats acetaminophen poisoning by binding the poisonous forms of acetaminophen that are formed in the liver. NAC is

used in the treatment of cancer, human immunodeficiency virus (HIV) infection, cardiovascular and respiratory diseases and neurodegenerative disorder.[1,15,16]

Acetaminophen (AC) or paracetamol is one of the important drugs used as analgesics and anti pyreticsin the treatment of mild to moderate pains associated with a headache, backache, arthritis and postoperative pain.[17-19] It has low toxicity at therapeutic doses but in the overdose, it causes liver and kidney damages which may lead to an acute liverfailure.[18] A complementary presence of AA intensifies the main favorable effect of AC and it is used in the prevention and treatment of acetaminophen–induced hepatotoxicity in man.[18]

Tryptophan (2–amino–3–(1H–indol–3–yl)–propionic acid; Trp) is an oxidizable amino acid to its crucial roles in biological systems and a vital constituent of proteins.[2,18] Due to its scarce presence in vegetables, this compound is sometimes added to diets, food products and pharmaceutical formulas. Trp has been implicated as a possible cause of schizophrenia when improperly metabolized.[18] Additionally, it is a precursor of the neurotransmitter serotonin and the brain serotonin availability depends upon the blood Trp levels.[2] Also, in the presence of AA, Trp forms an important chemical material in brain that called serotonin and scientists can control the production of serotonin in the body with determining Trp and AA concentration in animal blood.[18]

Based on mentioned subjects in above, simultaneous determination of electroactive species such as AA, LD, NAC, AC and Trp is particularly important, in the pharmaceutical and food industry and the diagnosis and monitoring of several disease.[17] Electrochemical analysis on the unmodified glassy carbon electrodes has limitations and hence often suffers from a pronounced fouling effect which results in rather a poor selectivity and reproducibility. Therefore, chemically modified electrodes (CMEs) have been usually used because lower the overpotential, increase

the reaction rate and sensitivity and improve selectivity.[4] A lot of chemically modified electrodes has been conducted based on nanoparticles, because their unique properties such as high electrical conductivity, high surface area and chemical stability.[1,20] Multi–walled carbon nanotubes (MWCNTs) are the most popular allotropes of carbon that have been utilized in electrochemical sensors and modify the electrodes for increase theelectronsconduction.[6,21] Moreover, various quinone derivatives have been studied as a modifier in chemically modified electrodes.[22-25] Quercetin (3,3',4',5,7–pentahydroxyflavone, see Scheme S1 for structure) is one of the most common flavonoids and a natural antioxidant present in the common human diets that it has beneficial effects on human health.[26] This compound has an *o*–hydroquinone moiety which it makes a good material for modification of electrodes.[26,27]

In the present work, a quercetin multiwall carbon nanotubes modified glassy carbon electrode, Q–MWCNT–GCE, prepared by electrochemical deposition of quercetin, Q, on a multi–walled carbon nanotube immobilized on the surface of a glassy carbon electrode. This modified electrode has good electrocatalytic effect for NAC electrooxidation. Additionally, the analytical performance of the Q–MWCNT–GCE sensor for the simultaneous determination of AA, LD, NAC, AC and Trp evaluate by differential pulse voltammetry (DPV). Q-MWCNT-GCE has excellent reproducibility and was successfully used for the voltammetric determination of AA, LD, NAC and AC in pharmaceutical samples.

2. Experimental

2.1. Reagents and apparatus

Ascorbic acid (AA) 99.7%, L–DOPA (LD) 99%, N–acetyl–L–cysteine (NAC) 99%, acetaminophen (AC) 99%, tryptophan (Trp) 99% and other reagents were purchased from Merck

Company and used without purification. AA tablet (500 mg AA per each tablet) from Hakim drugstore Co., Iran, LD tablet (100 mg LD per each tablet) from Desitin Co., Germany, NAC effervescent tablet (600 mg NAC per each tablet) from Darmanyab darou Co., Iran and AC tablets (325 mg AC per each tablet) from Jalinous Co., Iran were purchased from a local drugstore. The phosphate buffer solutions, PBS, (0.10 M) were made from H_3PO_4+NaH_2PO_4, and the pH was adjusted with 2.0 M NaOH. The pH was measured with a Metrohm model 691 pH/mV meters. Multiwall carbon nanotubes with characteristics of 10–20 nm in diameter, 5–20 mm long, and 95% pure were purchased from NanoLab Inc. (Brighton, MA). The electrochemical experiments were performed with a potentiostat/galvanostat PGSTAT 101 model from AutoLab (Ecochemie, Netherlands), with Nova 1.70 software and a conventional three–electrode cell. The working electrode was Q–MWCNT–GCE, and the reference electrode was a saturated calomel electrode (SCE). Also, a platinum electrode was used as the auxiliary one. All measurements were made at room temperature.

2.2. Electrodes preparation

The bare GCE (BGCE) was polished with alumina slurry using a polishing cloth then rinsed with doubly distilled water to produce a mirror like surface and sonicated in water for 5 min.1.0 mg MWCNT was dispersed in 1.0 mL DMF with the aid of ultrasonic agitation then for prepare the MWCNT–GCE, 1.0 μL of the black solution was cast onto the GCE surface and dried at room temperature for 15 min. Then, for preparation of Q–MWCNT–GCE, the MWCNT–GCE was rinsed with doubly distilled water and was placed in a 0.50 mM solution of quercetin in 0.10 M PBS (pH 7.0), and it was modified by 12 cycles of potential sweep between–0.10 and 0.50 V

at 20 mV s^{-1}. To fabricate the quercetin modified GCE (Q–GCE), the BGCE was placed in a 0.10 M phosphate buffer solution (pH 7.0) containing 0.50 mM of the quercetin and it was modified with the same procedure described for Q–MWCNT–GCE.

3. Results and discussion

3.1. Electrochemical behavior of Q–MWCNT–GCE

Fig. 1A, shows the cyclic voltammograms of the Q–MWCNT–GCE in a 0.10 M PBS (pH 7.0) at potential scan rates ranging from 15 to 100 mV s^{-1}. When the potential was scanned between –100 and 300 mV, a surface immobilized redox couple was observed with a formal potential ($E^{0'}$) value of 188 mV. In addition, the formal potential, $E^{0'}$, was almost independent of the potential scan rate for sweep rates ranging from 15 to 500 mV s^{-1}, suggesting facile charge transfer kinetics over this range of potential sweep rates. The plots of the anodic and cathodic peak currents as a function of the potential sweep rate show a linear relation (Fig. 1B) as predicted theoretically for a surface immobilized redox couple. The variation of the peak potentials versus the logarithm of the potential scan rate is shown in (Fig. 1C). The results show that the values of the anodic and cathodic peak potentials were proportional to the logarithm of the potential scan rate, and also $n\Delta E_p$ is higher than 0.20 V for the potential scan rates ranging from 800–1500 mV s^{-1} (Fig. 1D). Under these conditions, the surface electron transfer rate constant, k_s, and the charge transfer coefficient, α, for electron transfer between the electrodeposited quercetin and MWCNT–GCE can be estimated from the linear variation of the oxidation and the reduction peak potentials with the logarithm sweep rate according to the Laviron theory.[28] From the values of ΔE_p corresponding to different potential scan rates of 800 to

1500 mV s^{-1}, an average value of k_s was found to be 4.6±0.060 s^{-1} at pH 7.0. Also, the value of α was obtained 0.56. This value of k_s is comparable to those reported for a modifier that has a hydroquinone moiety.[18,27,29,30]

3.2. Effect of pH on the conditional formal potential of Q–MWCNT–GCE

The effect of pH on the voltammetric responses of Q–MWCNT–GCE was studied in PBS with pH values varying from 2 to 11 (Fig. 2). The pH dependence of the Q–MWCNT–GCE conditional formal potentials, $E^{0\prime}$, is given by the following equation:[31]

$$E^{0\prime} = E^{0} - \frac{2.303mRT}{nF}\text{pH} \qquad (1)$$

where E^0 is the standard redox potential, m and n are the number of protons and electrons involved in the redox reactions, and the other symbols have their usual meaning. Based on Eq. (1), for variation of $E^{0\prime}$ versus pH, the theoretical slope value of the linear segment is −59.2 mV/pH when m=n. As shown in the inset of Fig. 2, the conditional formal potential ($E^{0\prime}$) of the surface redox couple is pH–dependent with slope of −56.8 mV per unit which is close to the Nernstian slope (−59.2 mV/pH unit at 25 °C). $E^{0\prime}$ is calculated by the midpoint potential between the anodic and cathodic peaks, $E^{0\prime}=(E_{p.a}+E_{p.c})/2$. The results indicate that the number of the transferred protons and electrons in the redox processes of mixed valence Q–MWCNT on glassy carbon electrode are equal, a finding which is in agreement with those reported in the literature.[32-35]

3.3. Electrocatalytic oxidation of NAC at the Q–MWCNT–GCE surface

The ability of Q–MWCNT–GCE for the electrocatalytic oxidation of NAC was appraised by cyclic voltammetry (Fig. 3). As it can be seen, at the Q–MWCNT–GCE surface the electrocatalytic responses of 1.0 mM NAC solution appear at 185 mV (curve b), which is very close to that of the surface confined modifier, whereas the cathodic peak current has virtually decreased significantly reflecting the process of NAC oxidation is according to an E_rC_i catalytic (E_rC_i') mechanism. Under the same conditions, the cyclic voltammograms of 1.0 mM NAC solution at the Q–GCE (curve d), MWCNT–GCE (curve e), and BGCE (curve g) surfaces were obtained. Also, curve (c) and (f) shows the voltammogram Q–GCE and BGCE in 0.10 M PBS (pH 7.0) as supporting electrolyte. As it can be seen, the anodic peak potentials for the oxidation of NAC at Q–MWCNT–GCE (curve b), Q–GCE (curve d), and MWCNT–GCE (curve e) are about 185, 228, and 240 mV, respectively. Therefore, the peak potential of NAC oxidation at Q–MWCNT–GCE (curve b) shifted by about 43 and 55 mV toward the less positive values compared with those at Q–GCE (curve d) and MWCNT–GCE (curve e), respectively. Moreover, at BGCE no anodic peak observed. Also, there is an enhancement of the anodic peak current at the Q–MWCNT–GCE surface (curve b) relative to the values observed at the other various electrodes (Table 1). It should be noted that combination of MWCNT and quercetin in the structure of the modified electrodes causes an increase in the effective surface area of the modified electrode and, hence, an increase in the current response of the analyte. On the other hand, quercetin as a mediator of the electron transfer plays an effective role in decreasing of the NAC oxidation overpotential (curve d). A comparison of the oxidation responses of NAC at the different electrode surface (Table 1) indicates that a combination of MWCNT and quercetin improves the electrochemical characteristics of NAC oxidation.

The electrocatalytic oxidation of NAC at Q–MWCNT–GCE was also studied by electrochemical impedance spectroscopy, EIS. Fig. 4 represents the EIS results of BGCE (curve a), MWCNT–GCE (curve b), Q–GCE (curve c) and Q–MWCNT–GCE (curve d) in the presence of 1.0 mM $Fe(CN)_6^{3-}$ in the 0.1 M phosphate buffer solution (pH 7.0). The semicircle diameters of Nyquist plot reflect the electron transfer resistance (R_{ct}), which is related to the electron transfer kinetics of the redox probe at the surface of the electrode. Moreover, EIS showed an almost straight line, suggesting that the electrode reaction was only controlled by diffusion. As it can be seen, BGCE exhibited a straight line and a semicircular portion with small diameter (curve a). After modifying the GCE with MWCNT, the R_{ct} decreased dramatically which was reflected by the appearance of a substantial decrease in the diameter of the semicircular part (curve b). It indicates that high electron conduction MWCNT makes the electron transfer eraser. When the GCE modified with quercetin film, the R_{ct} increased which indicates that the quercetin layer hinders the diffusion of $Fe(CN)_6^{3-}$ towards the electrode surface. As compared with curve c, the R_{ct} decreased in curve d which demonstrate that deposition of MWCNT on GCE enhances the electron transfer between quercetin and GCE. Therefore, the MWCNT played an important role in promoting electrochemical performance of this modified electrode.

The effect of the potential scan rate on the electrocatalytic oxidation of NAC at the Q–MWCNT–GCE surface was used to obtain information about the oxidation mechanism of NAC. The linear sweep voltammograms of Q–MWCNT–GCE in a 0.10 M PBS (pH 7.0) containing 0.20 mM NAC at the different potential scan rates (Fig. S1A), were used to get the kinetic information about the rate–determining step of the NAC electrocatalytic oxidation at the modified electrode surface. As shown in Fig. S1B, the oxidation peak currents, I_p, of NAC increase linearly with the square root of the potential scan rate, $v^{1/2}$. This behavior indicates that

the nature of this redox process is diffusion-controlled. The number of electrons in the overall reaction of NAC electrocatalytic oxidation can be obtained from the slope of the I_p versus $v^{1/2}$ plots (Fig. S1B). According to the following equation for totally irreversible diffusion controlled processes:[36-39]

$$I_p=3.01\times10^5 n[(1-\alpha)n_\alpha]^{1/2}AC_bD^{1/2}v^{1/2} \quad (2)$$

and considering $(1-\alpha)n_\alpha=0.70$ (see below), $D=1.22\times10^{-6}$ cm^2 s^{-1} (obtained by chronoamperometry), $C_b=0.20$ mM of NAC, and $A=0.0314$ cm^2 (geometric surface area), it is estimated that the total number of electrons involved in the anodic oxidation of NAC is $n=1.8\cong2.0$. Also, the plot of the scan rate–normalized peak current ($I_p\ v^{-1/2}$) versus the potential scan rate exhibits characteristics of a typical E_rC_i' process (Fig. S1C).[37] Therefore, the oxidation mechanism of NAC at the proposed modified electrode is as follows:

$$Q \underset{}{\overset{k_s}{\rightleftharpoons}} Q_{(Oxidized\ form)} + 2H^+ + 2e^- \qquad E_r \quad (3)$$

$$Q_{(Oxidized\ form)} + NAC \xrightarrow{k} Q + NAC_{(Oxidized\ form)} \qquad C_i' \quad (4)$$

The theoretical model of Andrieux and Saveant[38] for an E_rC_i' mechanism, was used to obtain the electron transfer catalytic rate constant, k', between the modifier (quercetin here) and the analyte (NAC). Based on the Andrieux and Saveant theoretical model,[38] the following relation (Eq. (5)) exists between the peak current and the square root of potential scan rate, $v^{1/2}$.

$$I_{cat}=0.496nFAC_b(nFDv/RT)^{1/2} \quad (5)$$

where C_b is the bulk concentration (mol cm^{-3}) of the analyte. The relation holds true in the case of slow potential scan rate and large catalytic rate constant, k', between an analyte and a modifier. The values of heterogeneous rate constant, k', result in coefficient values lower than 0.496. At low potential scan rates, the value of this coefficient was found 0.26 for oxidation of NAC at the Q–MWCNT–GCE surface, considering $A=0.0314$ cm^2 and $D=1.22\times10^{-6}$ cm^2 s^{-1}

(obtained by chronoamperometry as below) in the presence of 0.20 mM of NAC. Using this value as well as Fig. 1 in the theoretical paper of Andrieux and Saveant,[38] an average value of k'=(6.5±0.08) $\times 10^{-4}$ cm s^{-1} was found for potential scan rates ranging from 2 to 8 mV s^{-1}. Fig. S1D, shows Tafel plots that were drawn from the data of the rising part of the current–voltage curves (known as Tafel region) recorded at the potential scan rates of 2, 4, 6 and 8 mV s^{-1} in a 0.10 M PBS (pH 7.0) containing 0.20 mM NAC. This part of the voltammogram is affected by the electron transfer kinetics between the substrate (NAC) and Q–MWCNT–GCE. The data of the Tafel plots can be used for evaluating kinetic parameters of the NAC electrocatalytic oxidation at the modified electrode surface. Based on the slope of the Tafel plots, the anodic electron transfer coefficient, α_a, between the modified electrode surface and NAC is obtained 0.30±0.010.[37] In addition, the exchange current density, J_0, appeared to be readily accessible from the intercept of the Tafel plots.[37] The average value of the exchange current density, J_0, was found as 0.110±0.003 μA cm^{-2} for NAC oxidation at the modified electrode surface.

3.4. Chronoamperometric studies

The diffusion coefficient of NAC in an aqueous PBS (pH 7.0), during its electrocatalytic oxidation at the Q–MWCNT–GCE surface, was calculated using chronoamperometry method. The chronoamperograms obtained at a potential step of 250 mV are depicted in Fig. S2. For an electroactive material (NAC in this case) with a diffusion coefficient of D, the current of the electrochemical reaction (at a mass transfer limited rate) was described by the Cottrell equation:[37]

$$I=nFAD^{1/2}C/(\pi^{1/2}t^{1/2}) \quad (6)$$

where D and C_b are the diffusion coefficient ($cm^2\ s^{-1}$) and the bulk concentration (mol cm^{-3}), respectively. Under diffusion control, the plot of I versus $t^{-1/2}$ will be linear and, from its slope, the value of D can be obtained. Such studies were carried out in various NAC concentrations at the Q–MWCNT–GCE surface. Fig. S2, inset A, shows the experimental plots with the best fits for different concentrations of NAC employed. The slopes of the resulting straight lines were then plotted versus the NAC concentration (Fig. S2, inset B), from whose slope a diffusion coefficient of 1.22×10^{-6} $cm^2\ s^{-1}$ was calculated.

3.5 Differential pulse voltammetric measurement

The analytical applicability of Q–MWCNT–GCE for the determination of NAC was examined using differential pulse voltammetry (DPV) method (Fig. 5). Since DPV has a much higher current sensitivity than cyclic voltammetry, it was used to estimate the lower limit of detection and the linear range of NAC. The results show the peak current of NAC electrooxidation at the Q–MWCNT–GCE surface was linearly dependent on the NAC concentration. Insets of (A) and (B) of Fig. 5 show clearly that the calibration plots are constituted from two linear segments with different slopes, correspond to two different ranges of 1.1–50.0 μM and 50.0–1000.0 μM of NAC. The lower detection limit of NAC, C_m, is obtained 0.44 μM using the equation $C_m=3s_{bl}/m$, where s_{bl} is the standard deviation of the blank response (μA) and m is the slope of the calibration plot (0.0475μA μM^{-1}) in the first linear range (1.1–50.0 μM).[39] The average voltammetric peak current and the precision estimated in terms of the coefficient of variation for 13 repeated measurements (n=13) of 10.0 μM of NAC at Q–MWCNT–GCE were obtained 2.0±0.050 μA and 2.5%, respectively. The obtained coefficient

variation value indicates that the modified electrode is stable and does not undergo surface fouling during the voltammetric measurements. In order to characterize the reproducibility of this sensor, a series of repetitive measurements were carried out in a 10.0 μM NAC solution. The data from four Q–MWCNT–GCE were prepared separately, have been obtained. Relative standard deviation (R.S.D.) of 3.1%was obtained in a 10.0 μM NAC, indicating that the modified electrode has excellent reproducibility and strong ability to prevent the electrode from fouling by the oxidation product. Some of the response characteristics obtained for NAC in this study are compared to those previously reported by others in Table S1.[1,15,40-48] A comparison of the analytical parameters of NAC determination at various modified electrode surfaces shows that the proposed modified electrode has advantages such as wide linear dynamic range (1.1–1000.0 μM) for NAC quantitative measurement.

3.6. Simultaneous differential pulse voltammetric determination of AA, LD, NAC, AC and Trp at the Q–MWCNT–GCE surface

DPV technique provides a better peak resolution and current sensitivity than cyclic voltammetry and is often used for simultaneous determination of different species in a mixture. One of the main objectives of this study was to introduce a modified electrode which would be used not only for the electrocatalytic oxidation of NAC but also for the successful separation of AA, LD, AC and Trp electrochemical responses into well–defined peaks. Fig. 6A shows the differential pulse voltammograms obtained for the oxidation of different concentrations of AA, LD, NAC, AC and Trp at Q–MWCNT–GCE. As it can be seen, at Q–MWCNT–GCE, there existed five well–distinguished anodic peaks at potentials of –20, 85, 195, 290 and 580 mV

corresponding to the oxidation of AA, LD, NAC, AC and Trp, respectively. Additionally, substantial increases in the peak currents were detected due to successive increases of AA, LD, NAC, AC and Trp in the analyte solution. The inset of Fig. 6A shows the differential pulse voltammogram of BGCE in a 0.10 M PBS (pH 7.0) containing of 700.0 μM of AA, 100.0 μM of LD, 30.0 μM of NAC, 50.0 μM of AC and 300.0 μM of Trp. This voltammogram indicates that a BGCE could not separate the analytical signals of AA, LD, NAC, AC and Trp. Moreover, Figs.6B–6F show that the calibration plots for AA, LD, NAC, AC and Trp are linear for the concentration ranges of 363.0–800.0 μM of AA, 50.0–112.0 μM of LD, 18.0–40.0 μM of NAC, 30.0–68.0 μM of AC and 167.0–368.0 μM of Trp. It is interesting to note that the sensitivities of the modified electrode to NAC in the absence and presence of AA, LD, AC and Trp are near to each other. It denotes the fact that the oxidation processes of AA, LD, NAC, AC and Trp at the Q–MWCNT–GCE surface are independent of one another. Thus, simultaneous or individual measurements of AA, LD, NAC, AC and Trp are possible without any interference in the proposed modified electrode surface.

3.7. Application of Q–MWCNT–GCE for determination of AA, LD, NAC, and AC in real samples

The utility of the proposed modified electrode for determining AA, LD, NAC and AC in pharmaceutical formulations was tested by a DPV method. The modified electrode was used to determine AA, LD, NAC, and AC concentrations in different tablets. For the measurement of AA, LD, NAC and AC in tablet samples, one AA tablet (500 mg), one LD tablet (100 mg), one NAC tablet (600 mg) and one AC tablet (325 mg) dissolved in 1000 mL of double distilled water separately, and were diluted 7, 14, 185 and 54 times with a 0.10 M PBS, respectively. Then, the

diluted sample solutions were placed in an electrochemical cell to determine their concentrations using the DPV method. The obtained results are listed in Table 2. To verify the validity of the results, the samples were spiked with certain amounts of AA, LD, NAC and AC at levels similar to those of the samples themselves. The results in Table 2 show that RSD% and recovery rates of the spiked samples were acceptable. The reliability of the proposed sensor was also evaluated by comparing the obtained results with those declared in the label of the pharmaceutical products Table 2). As the table suggests, the results obtained by a DPV method are in close agreement with the values declared on the labels of the samples. This suggests that the detection procedures have been free from any interference on the part of the sample matrix. In addition, the statistical t-test was performed to evaluate the accuracy of the different analytes determination at the proposed modified electrode. Based on the t–test, the experimental t values ($t_{exp.}$) corresponding to total values of AA, LD, NAC and AC in the real samples were obtained as 1.4, 1.9, 2.4 and 2.2, respectively. The critical t-value (t_{crit}) for two degrees of freedom at the 95% confidence level (p=0.05%) is 4.3. These results indicated the $t_{exp.}$ values are less than that the $t_{crit.}$ value. Thus, it is concluded that the matrix of the real samples does not make any interference in the determination of them at the proposed modified electrode.

4. Conclusions

A Q–MWCNT–GCE was prepared and applied for electrocatalytic determination of NAC. By cyclic voltammetry technique, the surface electron transfer rate constant, k_s, and the charge transfer coefficient, α, for the electron transfer between quercetin and MWCNT-GCE were estimated. The results show that the characteristics of electrocatalytic oxidation of NAC are

significantly improved at the Q–MWCNT–GCE surface in comparison with a bare or MWCNT GCE. The diffusion coefficient of NAC was calculated to be 1.22×10^{-6} cm^2 s^{-1} under experimental conditions, using chronoamperometric results. The electron transfer catalytic rate constant, k', the charge transfer coefficient, α, the number of electrons involved in the rate–determining step, n_α, and the overall number of electrons involved in the catalytic oxidation of NAC at the modified electrode surface were also determined. The detection limit of NAC was found to be 0.44 μM, and the calibration plots were linear within two ranges: 1.1–50.0 and 50.0–1000.0 μM of NAC. Also, the proposed modified electrode was used for the simultaneous determination of AA, LD, NAC, AC and Trp. Finally, this study has demonstrated the practical analytical utility of the modified electrode for the determination of AA, LD, NAC and AC in real samples.

References

1. H. R. Zare and F. Chatraei, *Sens. Actuators B: Chem.*, 2011, **160**, 1450-1457.
2. F. Chatraei and H. R. Zare, *Analyst*, 2011, **136**, 4595-4602.
3. J. Balamurugan, S. Senthil Kumar, R. Thangamuthu and A. Pandurangan, *J. Mol. Cat. A: Chem.*, 2013, **372**, 13-22.
4. H. R. Zare, M. Namazian and N. Nasirizadeh, *J. Electroanal. Chem.*, 2005, **584**, 77-83.
5. X. Zhang, Y. Cao, S. Yu, F. Yang and P. Xi, *Biosens. Bioelectron.*, 2013, **44**, 183-190.
6. A. Babaei, A. R. Taheri and I. Khani Farahani, *Sens. Actuators B: Chem.*, 2013, **183**, 265-272.
7. F. Kong, H. Liu, J. Dong and W. Qian, *Biosen. Bioelectron.*, 2011, **26**, 1902-1907.
8. F. R. F. Leite, C. M. Maroneze, A. B. de Oliveira, W. T. P. d. Santos, F. S. Damos and R. d. C. S. Luz, *Bioelectrochem.*, 2012, **86**, 22-29.
9. K. Min, T. Kathavarayan, K. Park and Y. J. Yoo, *J. Mol. Cat. B: Enzym.*, 2013, **90**, 87-90.
10. I. S. Pienaar and P. F. Chinnery, *Pharm.Ther.*, 2013, **137**, 1-21.
11. S. Fahn, *Ann.Neurol.*, 1992, **32**, S128-S132.
12. E. Palombo, L. J. Porrino, K. S. Bankiewicz, A. M. Crane, I. J. Kopin and L. Sokoloff, *Brain Res.*, 1988, **453**, 227-234.
13. S. Przedborski, V. Jackson-Lewis and S. Fahn, *Mov.Disord.*, 1995, **10**, 312-317.
14. H. U. Hink, N. Santanam, S. Dikalov, L. McCann, A. D. Nguyen, S. Parthasarathy, D. G. Harrison and T. Fukai, *Arterioscler.Thrombo.Vasc.Biol.*, 2002, **22**, 1402-1408.
15. M. Pournaghi-Azar and F. Ahour, *J. Electroanal. Chem.*, 2008, **622**, 22-28.
16. Z.-N. Gao, J. Zhang and W.-Y. Liu, *J. Electroanal. Chem.*, 2005, **580**, 9-16.

17. F. Chatraei and H. R. Zare, *Anal. Methods*, 2012, **4**, 2940-2947.

18. N. Nasirizadeh, Z. Shekari, H. R. Zare, S. A. Ardakani and H. Ahmar, *J. Braz. Chem. Soc.*, 2013, **24**, 1846-1856.

19. A. Kutluay and M. Aslanoglu, *Sens. Actuators B: Chem.*, 2013, **185**, 398-404.

20. H. R. Zare, S. H. Hashemi and A. Benvidi, *Anal.Chim.Acta*, 2010, **668**, 182-187.

21. T. Thomas, R. J. Mascarenhas, P. Martis, Z. Mekhalif and B. Swamy, *Mat. Sci. Eng. C*, 2013, **33**, 3294-3302.

22. H. R. Zare, Z. Sobhani and M. Mazloum-Ardakani, *Sens. Actuators B: Chem.*, 2007, **126**, 641-647.

23. M. Reza Shishehbore, H. R. Zare and D. Nematollahi, *J. Electroanal. Chem.*, 2012, **665**, 45-51.

24. H. R. Zare, M. R. Shishehbore and D. Nematollahi, *Electrochim. Acta*, 2011, **58**, 654-661.

25. H. R. Zare, N. Nasirizadeh, H. Ajamain and A. Sahragard, *Mat. Sci. Eng.: C*, 2011, **31**, 975-982.

26. J.-B. He, G.-P. Jin, Q.-Z. Chen and Y. Wang, *Anal.Chim.Acta*, 2007, **585**, 337-343.

27. J. B. Raoof, R. Ojani, M. Amiri-Aref and M. Baghayeri, *Sens. Actuators B: Chem.*, 2012, **166**, 508-518.

28. E. Laviron, *J. Electroanal. Chem.*, 1979, **101**, 19-28.

29. H. R. Zare, Z. Shekari, N. Nasirizadeh and A. A. Jafari, *Cat. Sci. Tec.,* 2012, **2**, 2492-2501.

30. H. R. Zare, F. Chatraei and N. Nasirizadeh, *J. Braz. Chem. Soc.*, 2010, **21**, 1977-1985.

31. H. R. Zare, M. Eslami, M. Namazian and M. L. Coote, *J. Phys. Chem. B*, 2009, **113**, 8080-8085.

32. M. Vuković, T. Valla and M. Milun, *J. Electroanal. Chem.*, 1993, **356**, 81-91.

33. A. S. Kumar and J. M. Zen, *Electroanal.*, 2004, **16**, 1211-1220.

34. C. C. Ti, Y. Umasankar and S. M. Chen, *Electroanal.*, 2009, **21**, 1855-1861.

35. P. Shakkthivel and S.-M. Chen, *Biosen.Bioelectro.*, 2007, **22**, 1680-1687.

36. S. Antoniadou, A. Jannakoudakis and E. Theodoridou, *Syn.Metals*, 1989, **30**, 295-304.

37. A. J. Bard and L. R. Faulkner, *Electrochemical methods: fundamentals and applications*, John & Wiley, New York, 2001.

38. C. Andrieux and J. Saveant, *J. Electroanal. Chem.*, 1978, **93**, 163-168.

39. H. R. Zare, N. Nasirizadeh, F. Chatraei and S. Makarem, *Electrochim. Acta*, 2009, **54**, 2828-2836.

40. W. Toito Suarez, L. H. Marcolino Jr and O. Fatibello-Filho, *Microchem. J.*, 2006, **82**, 163-167.

41. J. Raoof, R. Ojani, M. Amiri-Aref and F. Chekin, *J. Appl. Electrochem.*, 2010, **40**, 1357-1363.

42. J. B. Raoof, R. Ojani, F. Chekin, M. Jahanshahi and S. Rashid-Nadimi, *Electroanal.*, 2009, **21**, 2674-2679.

43. R. R. Moore, C. E. Banks and R. G. Compton, *Analyst*, 2004, **129**, 755-758.

44. D. R. d. Carmo, R. M. d. Silva and N. R. Stradiotto, *J. Braz. Chem. Soc.*, 2003, **14**, 616-620.

45. H. Heli, S. Majdi and N. Sattarahmady, *Sens. Actuators B: Chem.*, 2010, **145**, 185-193.

46. S. Shahrokhian, Z. Kamalzadeh, A. Bezaatpour and D. M. Boghaei, *Sens. Actuators B: Chem.*, 2008, **133**, 599-606.

47. A. A. Ensafi, H. Karimi-Maleh, S. Mallakpour and M. Hatami, *Sens. Actuators B: Chem.*, 2011, **155**, 464-472.

48. Y. Song, Z. He, F. Xu, H. Hou and L. Wang, *Sens. Actuators B: Chem.*, 2012, **166**, 357-364.

Legend of Scheme, Tables and Figures

Fig. 1. (A) Cyclic voltammetric responses of Q–MWCNT–GCE in a 0.10 M phosphate buffer solution (pH 7.0) at different potential scan rates. Numbers 1–18 correspond to potential scan rate of 15–100 mV s^{-1}, respectively. (B) Plots of the anodic and cathodic peak currents *vs.* the potential scan rate. (C) Variation of the peak potentials *vs.* the logarithm of the potential scan rate. (D) Magnification of the same plot for high potential scan rates.

Fig. 2. Cyclic voltammograms of Q–MWCNT–GCE (at 20 mV s^{-1}) in a 0.10 M phosphate buffer solution in different pHs (2.0–11.0). Inset shows the plot of formal potential, $E^{0\prime}$, *vs.* pH.

Fig. 3. Cyclic voltammograms of Q–MWCNT–GCE in a 0.10 M phosphate buffer solution (pH 7.0) at potential scan rate 20 mV s^{-1} in (a) the absence and (b) the presence of 1.0 mM NAC. (c) and (f) as (a) at Q–GCE and BGCE. (d), (e) and (g) as (b) at Q–GCE, MWCNT–GCE and BGCE, respectively.

Fig. 4. Nyquist plots of (a) BGCE, (b) MWCNT–GCE, (c) Q–GCE, and (d) Q–MWCNT–GCE in the presence of 1.0 mM $Fe(CN)_6^{3-}$ in the phosphate buffer solution (pH 7.0).

Fig. 5. Differential pulse voltammograms of Q–MWCNT–GCE in a 0.10 M phosphate buffer solution (pH 7.0) containing different concentrations of NAC. Numbers of 1–38 correspond to 1.1 to 1000.0 μM of NAC. Insets (A) and (B) show the plots of the electrocatalytic peak current as a function of NAC concentration in the concentration ranges of 1.1–50.0 μM and 50.0–1000.0μM of NAC, respectively.

Fig. 6. (A) Differential pulse voltammograms of Q–MWCNT–GCE in a 0.10 M phosphate buffer solution (pH 7.0) containing different concentrations of AA, LD, NAC, AC and Trp. Numbers 1–11 correspond to 363.0–800.0 μM of AA, 50.0–112.0 μM of LD, 18.0–40.0 μM of

NAC, 30.0–68.0 μM of AC and 167.0–368.0 μM of Trp. Inset shows differential pulse voltammogram of a mixed solution of 700.0 μM of AA, 100.0 μM of LD, 30.0 μM of NAC, 50.0 μM of AC and 300.0 μM of Trp at a BGCE. (B)–(F) show the plots of the electrocatalytic peak current as a function of AA, LD, NAC, AC and Trp concentrations, respectively.

Table 1. Comparison of electrocatalytic oxidation of NAC (1.0 mM) at the various electrode surfaces at pH 7.0

Table 2. Determination and recovery results of AA, LD, NAC and AC in different tablets at the Q–MWCNT–GCE surface.

Fig. 1.

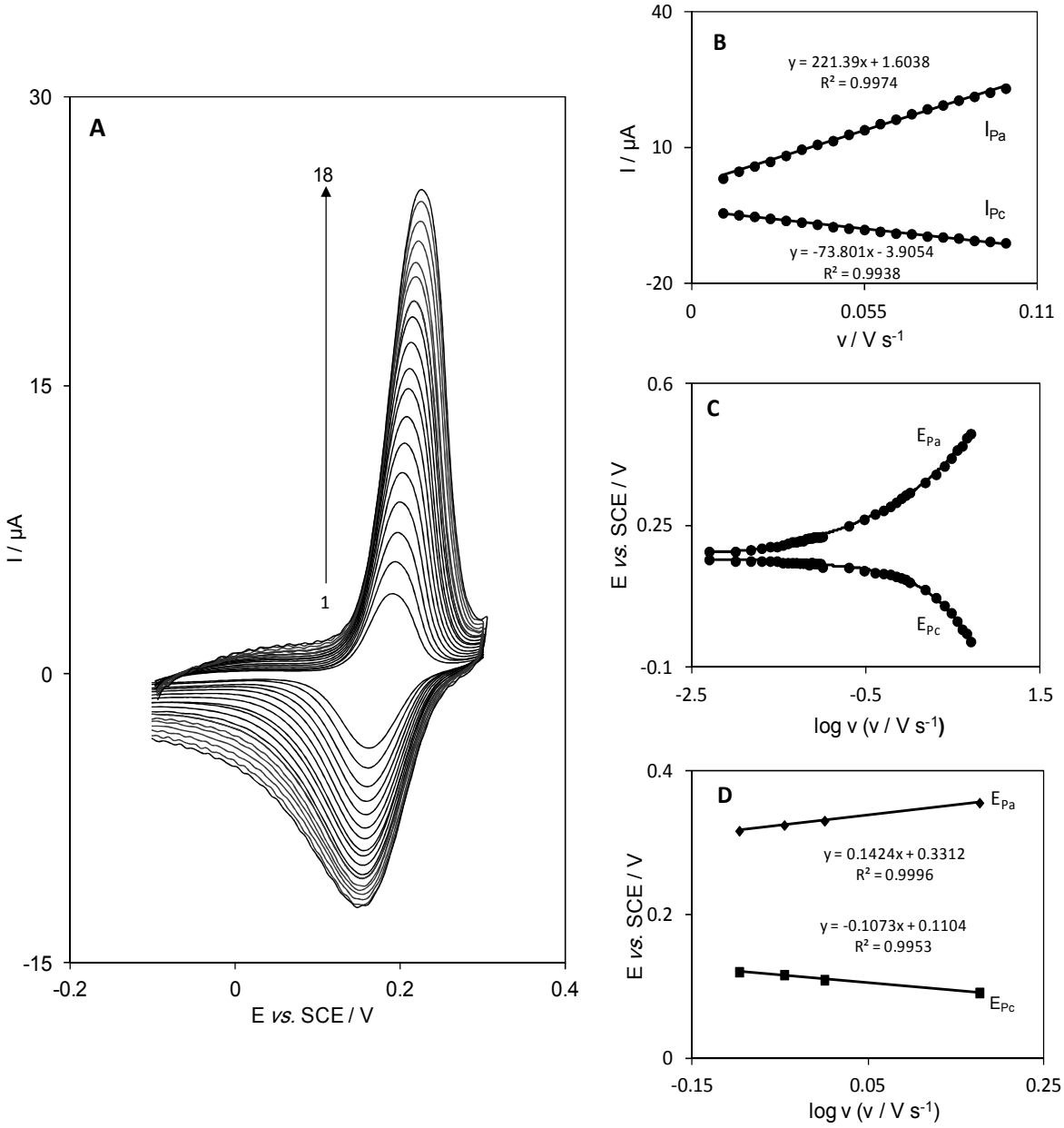

Fig. 2.

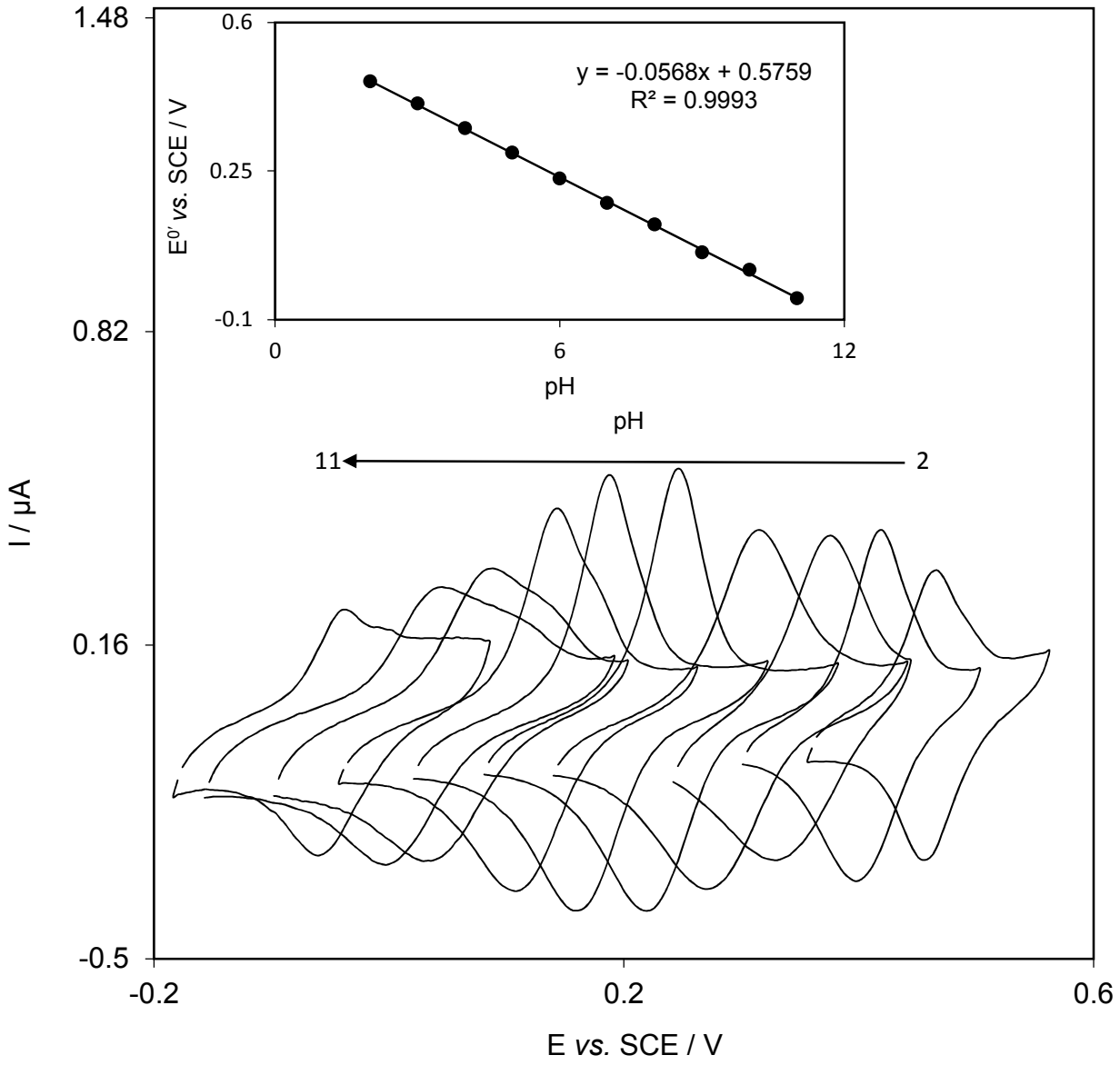

Fig. 3.

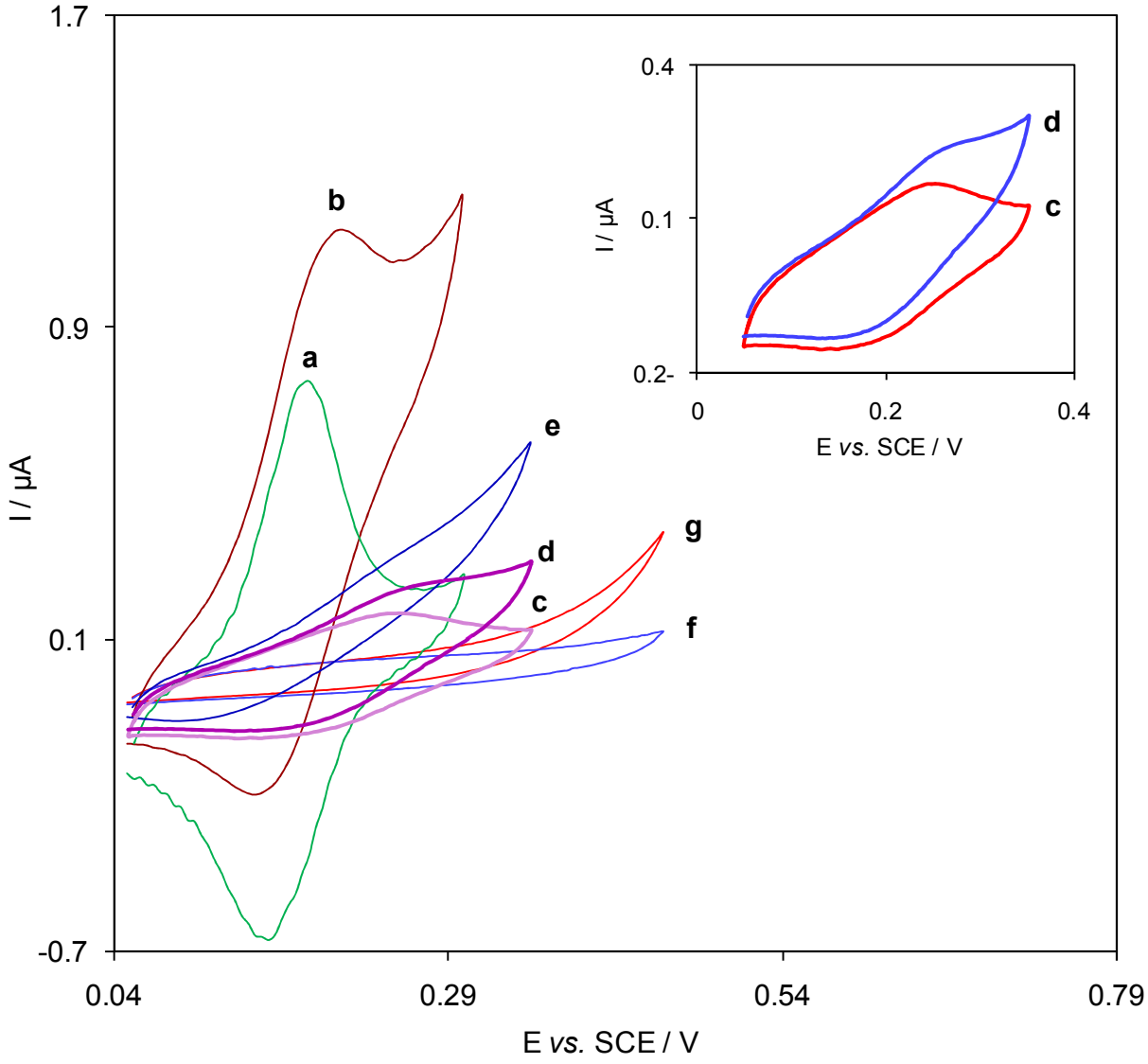

Fig. 4.

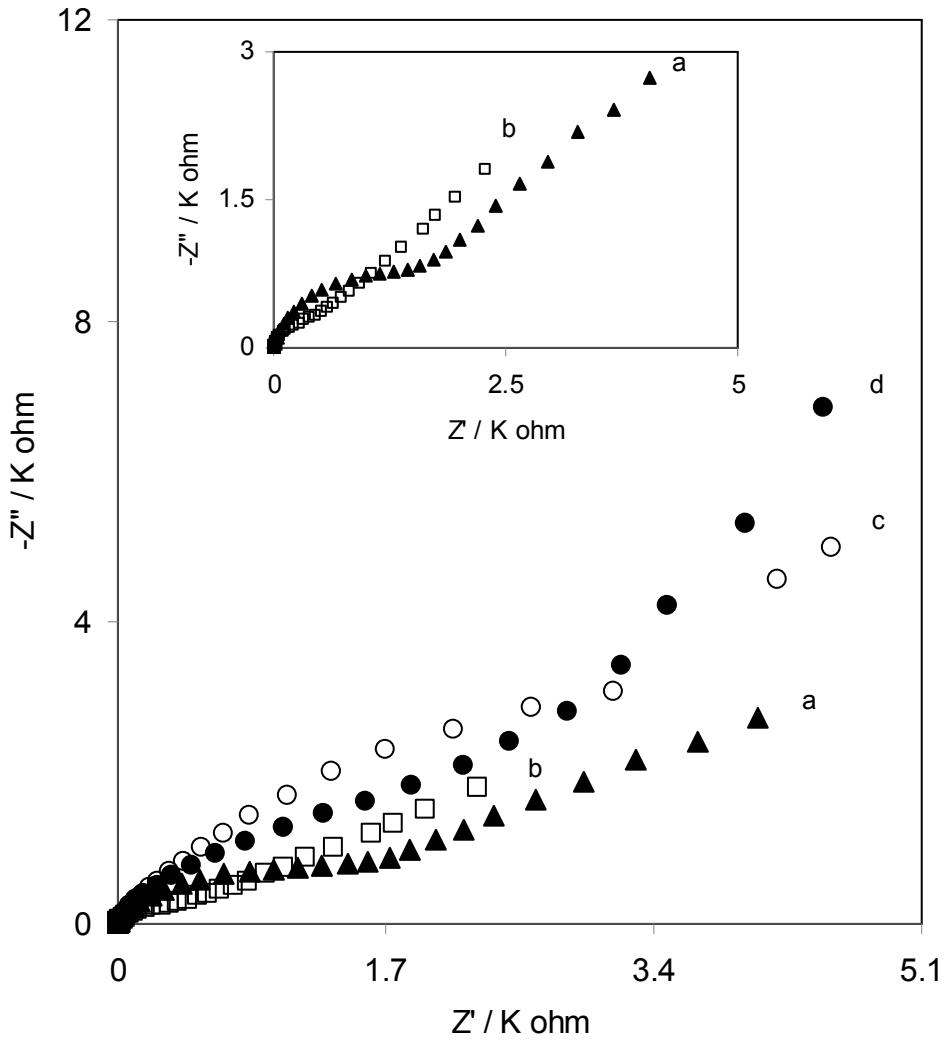

Fig. 5.

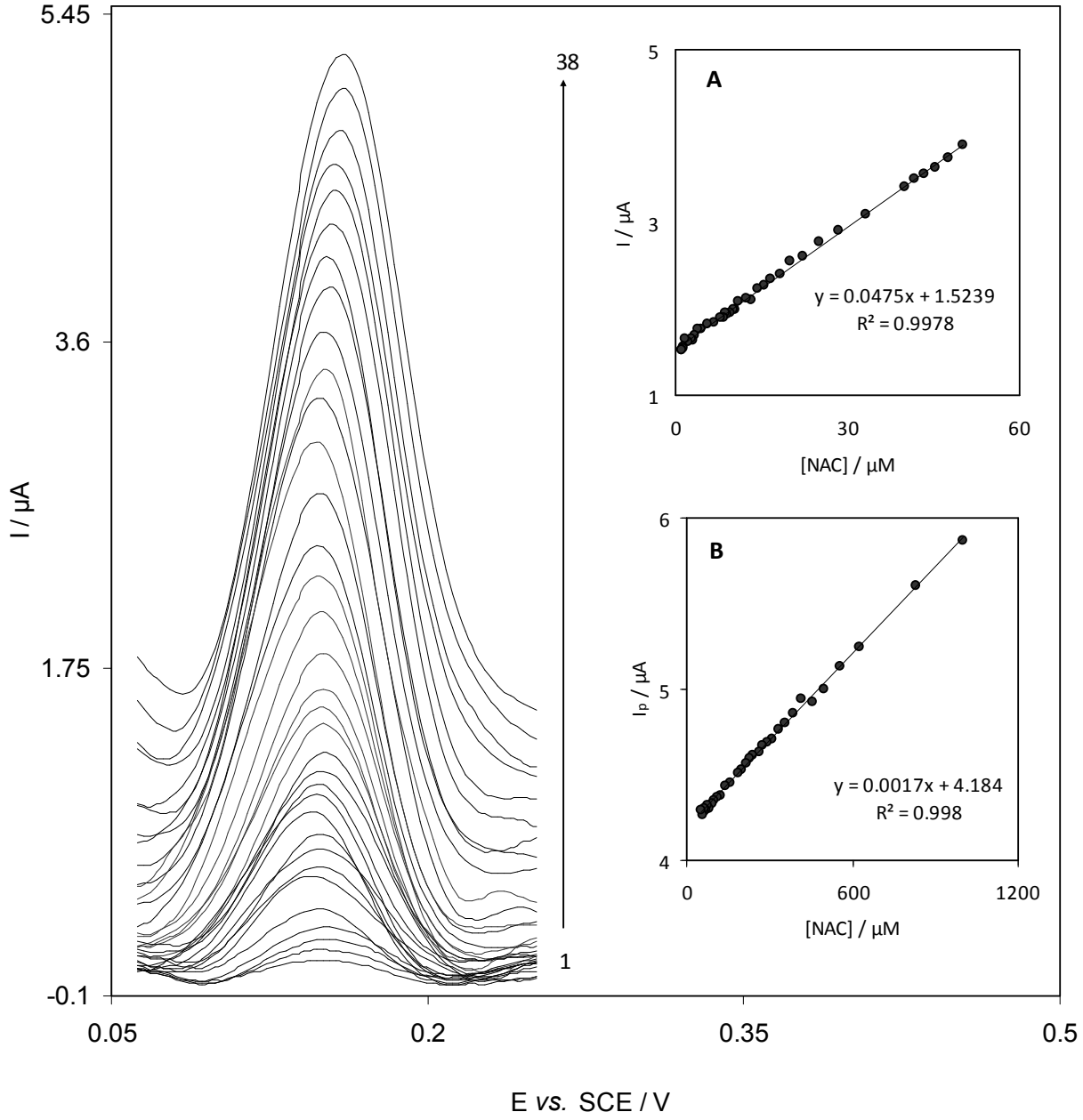

Fig. 6.

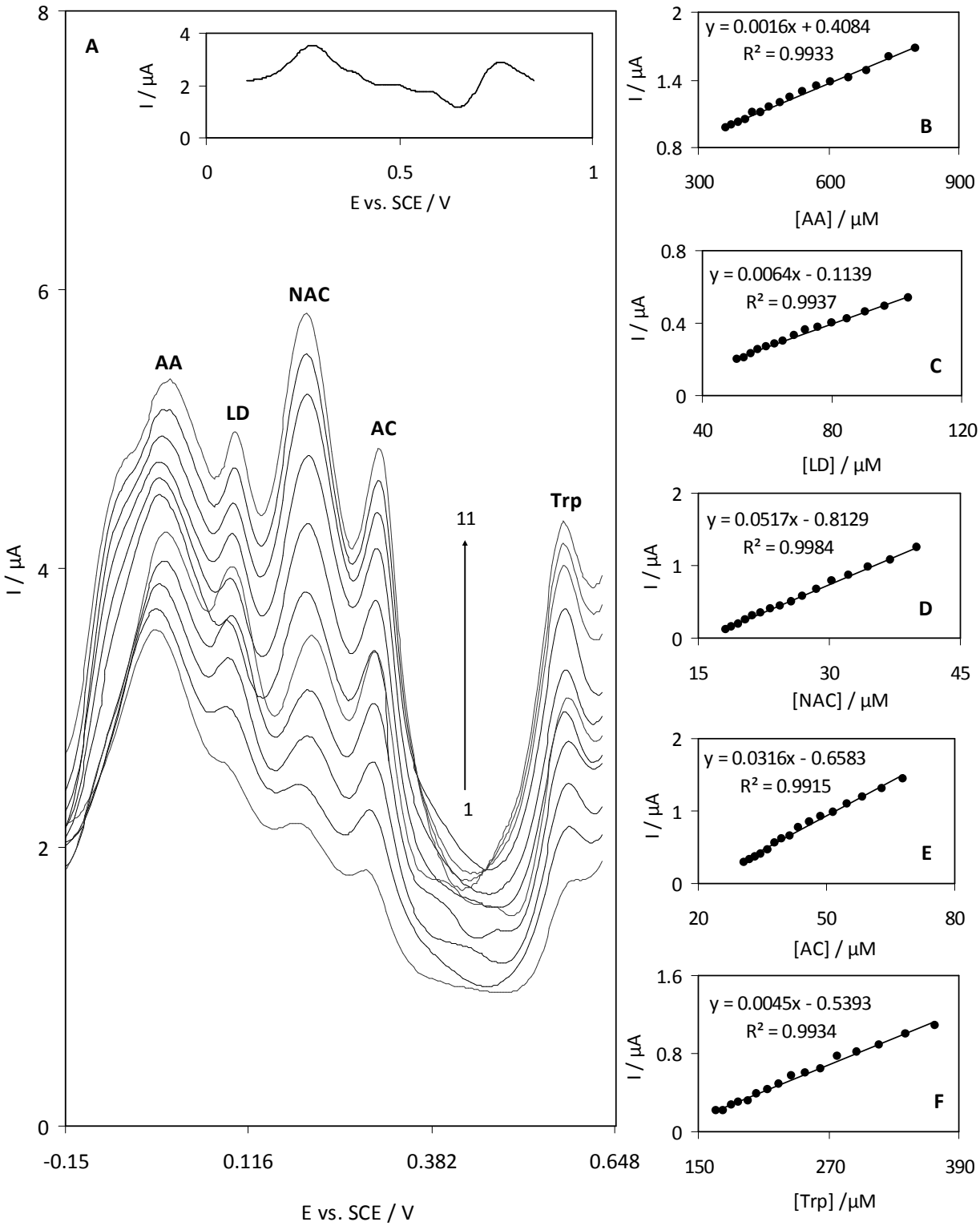

Table 1

Name of electrode[a]	Oxidation peak potential (mV)	Oxidation peak current(μA)
MWCNT–GCE	240	≅0.24
Q–GCE	228	0.11
Q–MWCNT–GCE	185	0.74

[a]MWCNT–GCE: Multi-wall carbon nanotubes modified GCE; Q–GCE: Quercetin modified GCE; Q–MWCNT–GCE: Quercetin multi-wall carbon nanotubes modified GCE.

Table 2

Samples[a]		Added (μM)				Found (μM)				RSD %				Recovery %				Total value[b,c] (mg)	Declared value[c] (mg)
Tablet of AA	AA	–	250.0	300.0	350.0	398.5	645.1	701.7	745.2	2.3	2.1	1.5	2.5	–	98.6	101.1	99.1	491.3±11.3	500.0
	LD	–	60.0	80.0	100.0	–	61.1	78.5	97.5	–	1.9	2.6	1.6	–	101.8	98.1	97.5		
	NAC	–	20.0	30.0	40.0	–	20.3	29.6	40.7	–	3.0	1.6	2.4	–	101.5	98.6	101.7		
	AC	–	35.0	50.0	65.0	–	34.2	50.6	64.1	–	1.8	2.1	2.8	–	97.7	101.2	98.6		
	Trp	–	200.0	250.0	300.0	–	202.2	248.5	302.6	–	1.7	2.4	2.5	–	101.1	99.4	100.8		
Tablet of L–DOPA	AA	–	400.0	500.0	600.0	–	389.5	505.1	579.1	–	1.9	2.3	1.5	–	97.4	101.0	96.5		
	LD	–	10.0	20.0	30.0	70.2	80.5	90.8	99.8	2.9	1.5	2.7	1.8	–	103.0	103.0	98.7	96.1±2.8	100.0
	NAC	–	25.0	30.0	35.0	–	25.3	29.1	35.9	–	2.3	1.9	2.1	–	101.2	97.0	102.6		
	AC	–	45.0	55.0	65.0	–	45.1	53.8	66.2	–	1.7	2.4	2.5	–	100.2	97.8	101.8		
	Trp	–	250.0	300.0	350.0	–	249.5	300.9	348.9	–	1.1	1.4	1.8	–	99.8	100.3	99.7		
Effervescent tablet of NAC	AA	–	450.0	600.0	750.0	–	451.0	599.2	751.6	–	1.2	2.2	2.6	–	100.2	99.9	100.2		
	LD	–	65.0	80.0	95.0	–	64.3	81.4	94.1	–	3.0	2.4	1.5	–	98.9	101.7	99.1		
	NAC	–	5.0	10.0	15.0	20.5	25.6	30.4	35.4	2.2	1.1	1.2	2.0	–	102.0	99.0	99.3	618.9±13.6	600.0
	AC	–	35.0	40.0	45.0	–	34.1	40.9	44.8	–	2.3	2.0	1.9	–	97.4	102.2	99.6		
	Trp	–	170.0	190.0	210.0	–	170.6	185.0	210.5	–	2.4	1.9	1.6	–	100.3	97.4	100.2		
Tablet of AC	AA	–	400.0	600.0	800.0	–	410.0	590.1	809.9	–	1.2	1.8	1.5	–	102.5	98.4	101.2		
	LD	–	55.0	85.0	110.0	–	56.2	84.1	109.5	–	2.3	2.9	1.9	–	102.2	98.9	99.5		
	NAC	–	20.0	25.0	30.0	–	20.2	24.5	30.6	–	1.5	2.0	1.2	–	101.0	98.0	102.0		
	AC	–	10.0	15.0	20.0	41.1	51.2	56.0	61.2	2.5	2.6	1.7	2.8	–	101.0	99.3	100.5	335.5±8.4	325.0
	Trp	–	190.0	240.0	290.0	–	188.9	243.0	281.1	–	1.1	2.1	1.5	–	99.4	101.2	96.9		

[a]AA: Ascorbic acid; LD: L-DOPA; NAC: N–acetyl–L–cysteine, AC: Acetaminophen; Trp: Tryptophan, [b]Three replicate measurements were made on the same samples. [b]The total values (average of three measurements) were obtained by multiplying the measured values by the appropriate dilution factor, [c]The value per each tablet.

Graphical Abstract

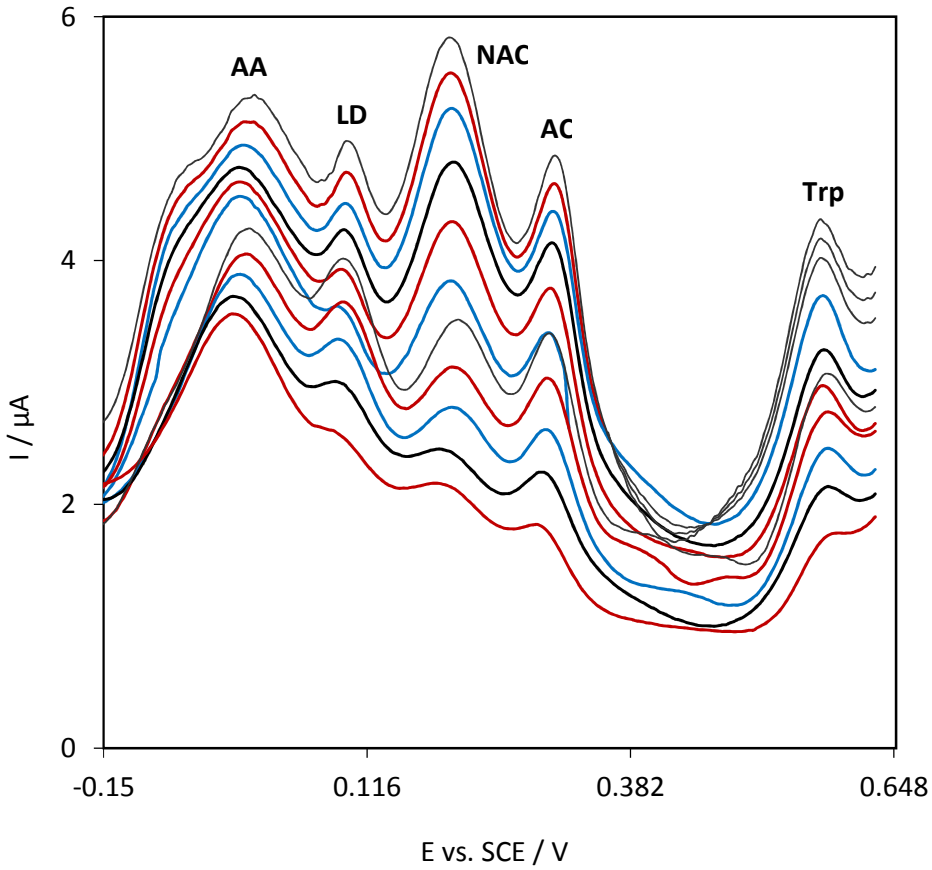

Quercetin MWCNT modified GCE was successfully used for N–acetyl–L–cysteine (NAC) electrocatalytic oxidation and simultaneous determination of ascorbic acid, L–DOPA, NAC, acetaminophen and tryptophan.